

# A Compact ACS-Fed Mirrored L-Shaped Monopole Antenna with SRR Loaded for Multiband Operation

Rengasamy Rajkumar\* and Kommuri Usha Kiran

**Abstract**—In this paper, a compact asymmetric coplanar strip (ACS)-fed mirrored L-shaped monopole antenna is presented. The proposed design consists of three mirrored L-shaped branches and a split ring resonator (SRR) loaded beneath the substrate, which are responsible for achieving multiband characteristics, compactness and good impedance matching. The proposed antenna with a compact dimension of  $22 \times 16.08 \times 1.6 \text{ mm}^3$  is fabricated and tested. The experiment result indicates that the proposed design, having  $-10 \text{ dB}$  impedance bandwidth of 200, 670 and 530 MHz for 2.44, 5.3 and 8.2 GHz, respectively, covers 2.4/5.2/5.8 GHz WLAN, 5.5 GHz WiMAX and 8.2 GHz ITU band. It has good radiation characteristics for both  $E$ -plane and  $H$ -plane in all the desired frequency bands and produces good performances compared to the existing antenna designs in the literature. The loaded SRR structure performance is validated through negative permeability extraction and various parametric studies.

## 1. INTRODUCTION

Presently, swift progress in modern wireless systems increases the demand of integrating various wireless applications in a single device. The multiband antenna is the most important technique which is able to cater to the modern communication demands with ease. Various multiband antenna methods have been proposed to achieve different wireless applications [1–6]. The aforementioned techniques occupy large space or have complex structures. To achieve compact and multiband characteristics in a single device, asymmetric coplanar strip (ACS) method is used. ACS method has a single ground plane instead of double ground planes as in the coplanar waveguide (CPW) fed technique, and it possesses all the advantages of the CPW technique. These features make ACS-fed antenna method suitable for easy integration and better size reduction process [7]. Various ACS-fed antenna techniques have been proposed to achieve the multiband characteristics [8–16]. Multiband performances were achieved by etching various shaped slots in the radiating element or ground plane of the antenna design in [8–11], by adding various shaped strips with the radiating element [12–15] and using loaded capacitance termination technique for dual-band performance in [16].

To achieve more size reduction in the antenna design, metamaterial based technique is considered. Metamaterials are artificial materials which have special properties such as negative permittivity and negative permeability. By using these properties, radiation characteristics such as bandwidth enhancement, size reduction and notch performance can be achieved in microwave devices [17–19]. A conductor backed ACS-fed design was proposed for multiband operation in [20], but it covers only Wireless Local Area Network (WLAN) band. Very few literatures are present in combination of ACS based models with SRR. In [21], SRR was etched on the radiating element of an ACS-fed antenna for achieving WLAN/Worldwide Interoperability for Microwave Access (WiMAX) applications, but it does not cover the International Telecommunication Union (ITU) band.

---

Received 15 March 2016, Accepted 21 May 2016, Scheduled 1 June 2016

\* Corresponding author: Rengasamy Rajkumar (imesanai@gmail.com).

The authors are with School of Electronics Engineering, VIT University, Chennai, Tamilnadu, India.

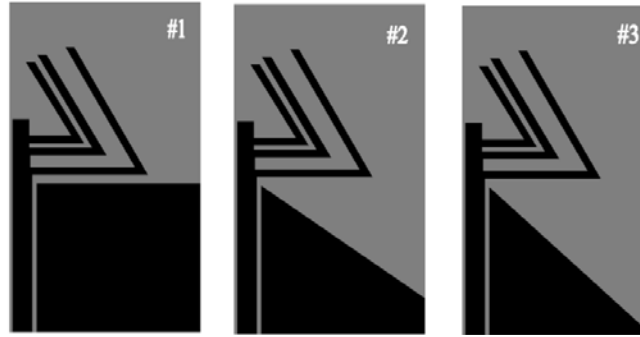


**Figure 1.** Evolution stages of the proposed multiband antenna.

In [8–16] and [20, 21], ACS-fed antenna designs cover either WLAN or WLAN/WiMAX or WLAN/ITU band. To cover the WLAN/WiMAX/ITU applications simultaneously, an additional antenna is required which increases the size of the overall system with additional cost.

In this article, a compact SRR loaded multiband antenna is proposed for multiband operation. A monopole antenna with mirrored L-shaped branches along with tapered ground plane is used as a radiating element. To achieve more size reduction and enhancement in bandwidth at higher frequencies, a rectangular SRR structure is loaded at the back side of the antenna. The proposed design covers wireless local area network (WLAN) 2.4/5.2/5.8 GHz and worldwide interoperability for microwave access (WiMAX) 5.5 GHz along with (ITU) 8.2 GHz simultaneously. It has a compact structure and better radiation characteristics in the desired frequency bands.

## 2. PROPOSED ANTENNA DESIGN

The proposed ACS-fed multiband antenna geometry is depicted in Figure 2, and flame retardant grade-4 (FR-4) substrate with dielectric constant of 4.4 and height of 1.6 mm is used. The antenna has a compact size of  $22 \times 16.08 \times 1.6 \text{ mm}^3$  and is fed by ACS-fed line with signal width of ( $F_w$ ) of 1.10 mm and gap ( $G$ ) of 0.3 mm between ACS fed line and ground plane which has  $50 \Omega$  impedance.

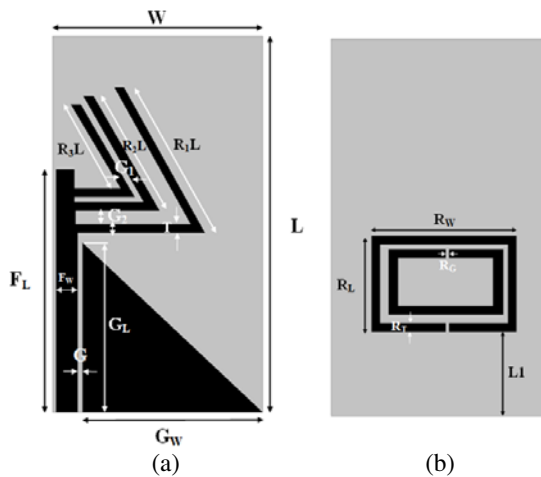


**Figure 2.** Geometry of the ACS-fed multiband antenna, (a) front and (b) back side.

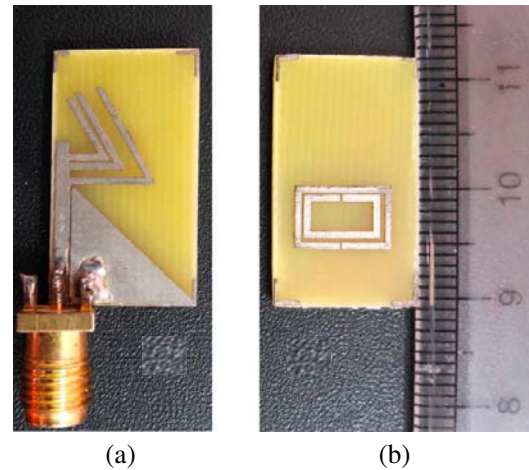


**Figure 3.** Photograph of the fabricated ACS-fed antenna, (a) front and (b) back side.

The characteristic impedance of the ACS-fed line is calculated [22] by using equations below

$$Z_0 = \frac{60\pi}{\sqrt{\varepsilon_{eff}}} \frac{K(k)}{K(k^1)} \quad (1)$$

$$K = \frac{a}{b} \quad (2)$$

$$k^1 = \sqrt{1 - k^2} \quad (3)$$

and  $\frac{K(K)}{K(k^1)}$  is the elliptical integral of first kind which is given by

$$\frac{K(K)}{K(k^1)} = \begin{cases} \frac{\pi}{\ln \frac{2(1 + \sqrt{k^1})}{(1 - \sqrt{k^1})}} 0 \leq k \leq \frac{1}{\sqrt{2}} \\ \frac{1}{\pi \ln \frac{2(1 + \sqrt{k})}{(1 - \sqrt{k})}} \frac{1}{\sqrt{2}} \leq k \leq 1 \end{cases} \quad (4)$$

$$\varepsilon_{eff} = 1 + \frac{\varepsilon_r + 1}{2} \quad (5)$$

Three different mirrored L-shaped branch strips are added with the ACS-fed monopole antenna. The branch length and position are optimized to obtain multiband characteristics. The fully tapered ground plane is used to achieve a broader bandwidth and better impedance matching. The rectangle-shaped SRR is employed at the back of the proposed antenna to obtain size reduction as well as to improve the impedance matching in the upper frequency region.

**Table 1.** Antenna parameters and their dimensions.

Parameters	Dimensions (mm)
$G_W, F_L, F_W, W$	10.90, 14.20, 1.10, 16.08
$L1, L, T, h, G, G_L,$	4.9, 22, 0.3, 1.6, 0.3, 9.9
$G_1, G_2, R_W, R_L, R_G$	0.3, 0.80, 8.6, 5.6, 0.2
$R_T, R_1L, R_2L, R_3L$	0.5, 9.81, 7.81, 5.81

The proposed antenna parameters are fixed based on the parametric analysis method and tabulated in Table 1. Photographs of the fabricated ACS-fed antenna (front side and back side) are shown in Figure 3.

### 3. RESULTS AND DISCUSSION

The electromagnetic simulator Ansoft HFSS V.14.0 is used to analyze the antenna design performance which works based on FEM solver. Evolution stages of the proposed antenna are depicted in Figure 1, and their reflection coefficients are shown in Figure 4. In Antenna #1, the conventional rectangle-shaped ground plane is used. It has three resonance frequency bands at 3.2, 4, 7.5 GHz, but these bands do not fall in the desired frequency region.

To achieve better performance and cover the desired application frequencies, a semi-tapered ground plane (Antenna #2) is used. Although the impedance matching is improved (#2) in Figure 4, it does not cover 2.4, 5 GHz bands but covers 8.2 GHz band partially. To cover all the desired applications, fully tapered ground plane is proposed as displayed in Figure 1 (#3). Due to tapering, the inductance reduces, which shifts the resonance of 2.4, 8.2 GHz and enhances the impedance matching at 5 GHz as shown in Figure 4 (#3).

Figure 5 shows simulated reflection coefficient of the proposed antenna with and without SRR structure. We observe that without SRR structure, the antenna resonates at 2.94, 3.9, 4.5 and 8.1 GHz.

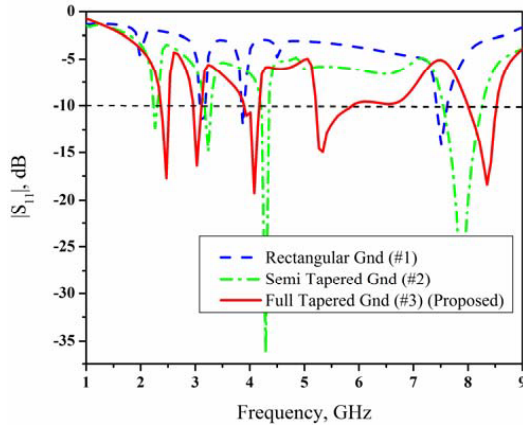


**Figure 4.** Simulated reflection coefficient of the evolution stage.

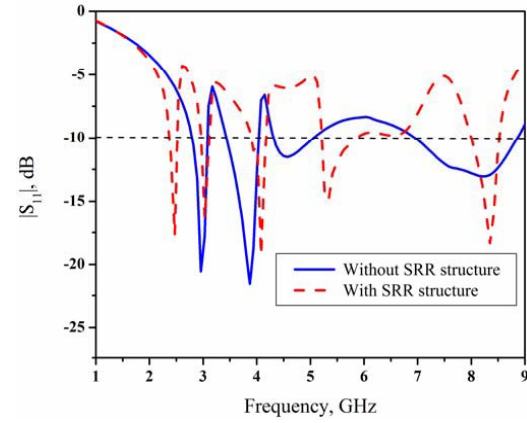


**Figure 5.** Simulated reflection coefficient of the proposed antenna with and without SRR structure.

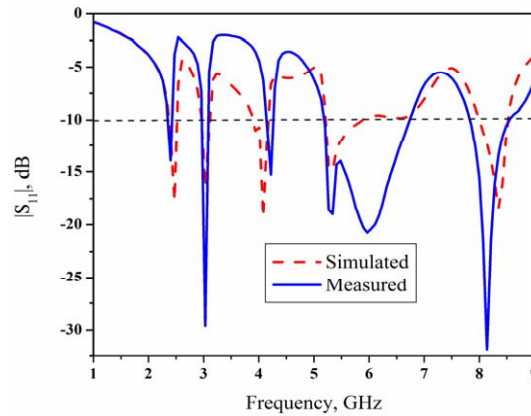


**Figure 6.** Simulated and measured reflection coefficient of the ACS-fed antenna.

It covers only ITU application effectively, and remaining applications are not covered properly. When the antenna is employed with the rectangle-shaped SRR on the back side of the substrate, performance enhancement such as size reduction, bandwidth enhancement and creating notch can be observed. The first resonance frequencies of the antenna with and without SRR structure are 2.44 and 2.9 GHz, respectively. It is observed that size reduction is achieved in the antenna with SRR structure. The rectangular SRR which has resonance around 7.4 GHz impacts the reflection coefficient of the antenna without SRR due to which the 5 GHz band is obtained in the proposed model. The last resonance bandwidth is reduced due to notch effect at 7.4 GHz. But, with SRR structure design covers the desired ITU band (8.05–8.50 GHz) completely. The placement position of rectangular SRR and its resonance frequencies are explained in Sections 4 and 5, respectively.

Simulated and measured reflection coefficients of the proposed ACS-fed multiband antenna are illustrated in Figure 6. It is observed that there are some deviations present among simulated and measured results due to the presence of dielectric losses in the substrate and soldering heat effects. The proposed design covers 2.3–2.53 GHz, 5.18–5.85 and 8–8.53 GHz. It can be used for 2.4/5.2/5.8 GHz (IEEE 802.11 a/b/g) WLAN, 5.25–5.85 GHz WiMAX and 8.05–8.50 GHz ITU band applications.

#### 4. PARAMETRIC STUDY FOR THE PROPOSED ANTENNA STRUCTURE

The proposed antenna performance has impact on various antenna parameters. Here, a few important parameters such as strip gap ( $G2$ ), position of SRR ( $L1$ ), split width of SRR ( $RG$ ) and outer branch

strip length ( $R_1L$ ) are investigated, and their simulated results are shown in Figures 7–10. The effect of varying parameter  $G2$  from 0.4 to 0.8 mm is depicted in Figure 7. At  $G2$  of 0.4 mm, the first and last resonance frequency bands' reflection coefficients are around  $-10$  dB and  $-18$  dB, respectively, but, both do not cover 2.4 and 8 GHz bands completely due to less coupling effect.

When the strip gap ( $G2$ ) is 0.6 mm, it covers the required reflection coefficient characteristics in the lower and middle bands, but it does not cover the entire frequency bandwidth of ITU band.  $G2$  of 0.8 mm covers all the desired applications including complete ITU band. Due to the high capacitive effect of the gap, the resonance band shifts to higher band and covers the entire ITU band (8.05–8.50 GHz).

In the proposed antenna design, an SRR is employed at bottom of the substrate, and its position is fixed based on the parametric study of  $L1$  from 11.9 to 4.9 mm as depicted in Figure 8. For  $L1$  of 11.9 mm, the impedance matching is very poor at 2.4 and 8.2 GHz frequency region. When the length is 9.9 mm, the impedance matching is enhanced compared to  $L2$  of 11.9 mm due to the coupling effect.

It produces desired performances at higher frequency band but does not cover the 2.4 GHz band. At  $L1$  of 4.9 mm, it covers all of the desired frequencies such as 2.4, 5 and 8.2 GHz with enough bandwidth. When the position of SRR is exactly beneath the third branch strip of the top layer, more coupling effect is present. Hence the position of SRR structure is fixed as  $L1$  of 4.9 mm.

Similarly, SRR's split width gap ( $RG$ ) is varied from 0.6 to 0.2 mm and analyzed, and their reflection coefficient performance is depicted in Figure 9.  $RG$ s of 0.6 and 0.4 mm produce similar resonance characteristics in all the frequency bands. They cover lower, middle and higher frequency bands but fail to cover the entire desired frequency (2.4–2.48, 5–5.85, 8.05–8.50 GHz) bandwidths. When  $RG$  is 0.2 mm, it is able to cover the entire WLAN (2.4, 5.2, 5.8 GHz), WiMAX (5.5 GHz), ITU band (8.2 GHz)

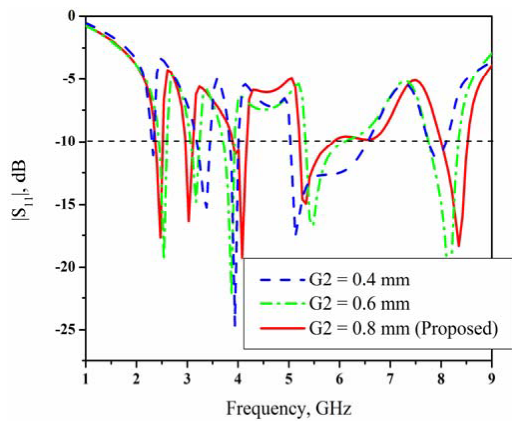


**Figure 7.** Reflection coefficients for various ' $G2$ ' values of antenna '#C'.

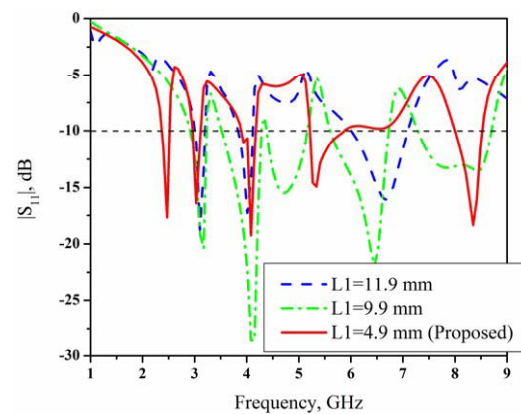


**Figure 8.** Reflection coefficients for various ' $L1$ ' values of antenna '#C'.

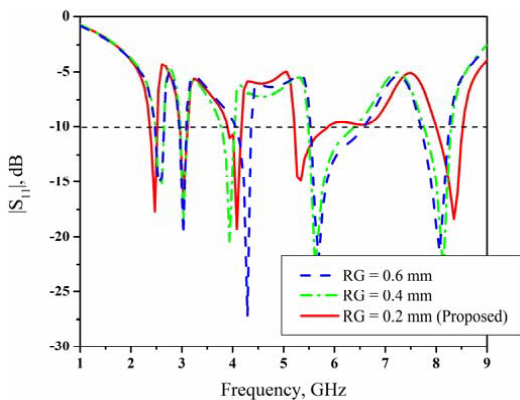


**Figure 9.** Reflection coefficients for various ' $RG$ ' values of antenna '#C'.

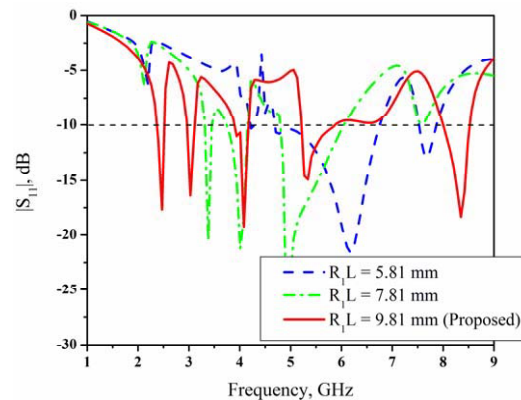


**Figure 10.** Reflection coefficients for various ' $R_1L$ ' values of antenna '#C'.

**Table 2.** Comparison of various existing ACS-fed antenna's with the proposed antenna.

S.No	References	Antenna size (mm <sup>2</sup> )	Total size occupied by antenna	Frequency bands covered by antenna (GHz)	Antenna Type	Average gain (dBi)
1	8	27.5 × 13	357.3	2.4/3.5/5.2/5.5/5.8	Tri-band	1.67
2	9	31 × 15	465	2.4/5.2/5.8	Tri-band	3.07
3	10	35 × 19	665	2.4/3.5/5.2/5.5/5.8	Tri-band	2.9
4	11	22 × 12	264	2.4/3.5/5.8	Tri-band	1.94
5	12	21 × 19	399	2.4/5.2	Dual band	1.8
6	13	26.5 × 12	318	2.4/3.5/5.8	Tri-band	2.01
7	14	13.4 × 22.7	304	2.5/4.9/5.2/5.5/5.8	Dual band	3
8	15	26 × 14	364	2.4/2.5/5.2 and 8	Tri-band	----
9	16	17 × 12	204	2.4/5.8	Dual band	2.01
10	20	25 × 17.5	437.5	2.4/5.2/5.5/5.8	Dual band	1.67
11	21	32 × 12	384	2.4/2.5/3.5/5.2/5.5/5.8	Tri-band	3.15
12	Proposed	22 × 16.08	353.76	2.4/5.2/5.5/5.8/ 8.2	Multiband	1.29

applications with enough bandwidth. As RG is smaller, the capacitive effect is higher which leads to necessary shifts in all the frequency bands compared to the RG values of 0.4 and 0.6 mm.

First branch strip length ( $R_1L$ ) is analyzed for various lengths from 5.81 to 9.81 mm as shown in Figure 10.  $R_1L$  of 5.81 and 7.81 mm has three resonance frequency bands. Both lengths do not cover all the desired applications (2.4, 8.2 along with 5 GHz) simultaneously.  $R_1L$  of 9.81 mm has good impedance matching and more coupling effect. It covers all the required application simultaneously. It is inferred that when  $R_1L$  increases, the electrical length tends to increase which shifts resonance frequency to the lower frequency band and aids in improving the impedance matching.

Table 2 represents various antenna parameters such as antenna size, total area occupied by the antenna, covered application bands, antenna type and average antenna gain of the existing literatures and the proposed antenna design.

From Table 2, we can conclude that the proposed antenna produces better performances in antenna size and covering application bands than the existing literatures. Though the proposed antenna has good results in all the parameters, it has less gain owing to its very small structure.

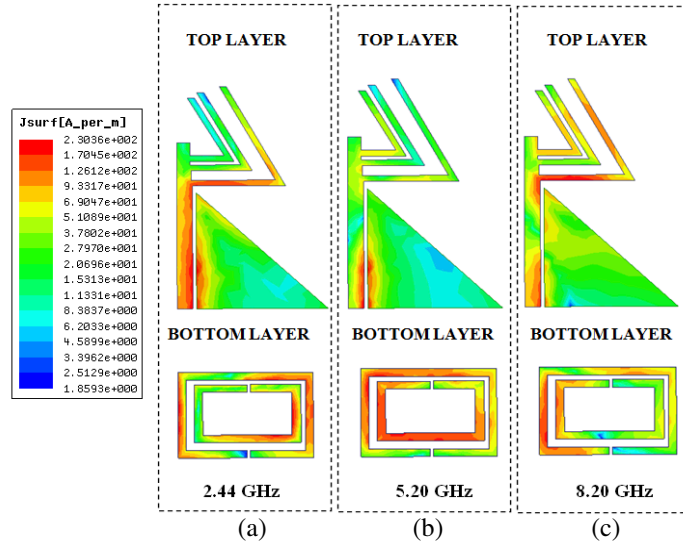
In order to get depth analysis of the proposed antenna multiband operation, simulated surface current distribution is carried out for various frequencies at 2.44, 5.2 and 8.2 GHz as depicted in Figures 11(a)–11(c).

Figure 11(a) represents the first resonance frequency at 2.44 GHz, and the current is concentrated more on the lower branch and along the monopole, whereas more current is distributed right and left side of outer ring and lower side of the inner ring. For 5.2 GHz, less current is concentrated along the monopole and more current concentrated at inner and outer rings of the SRR as depicted in Figure 11(b). At 8.2 GHz, currents are evenly distributed in all three strips of the antenna and less concentrated along monopole, whereas more current is concentrated on the left side of inner and outer rings of the SRR as shown in Figure 11(c). From the above analysis, we understand that three frequency bands are independent from each other.

## 5. RETRIEVING NEGATIVE PERMEABILITY OF SRR

In general, the split ring resonator and complementary split ring resonator possess special properties such as negative permeability and negative permittivity. To confirm the presence of negative permeability characteristics in the proposed SRR structure, the retrieval of reflection coefficient ( $S_{11}$ ) and transmission coefficient ( $S_{21}$ ) on the classic waveguide method [23] is used as depicted in Figure 12.

The proposed rectangular SRR structure is placed inside waveguide on the FR-4 substrate. Here,



**Figure 11.** Simulated surface current distributions of the proposed antenna at (a) 2.44 GHz, (b) 5.2 GHz, and (c) 8.2 GHz.

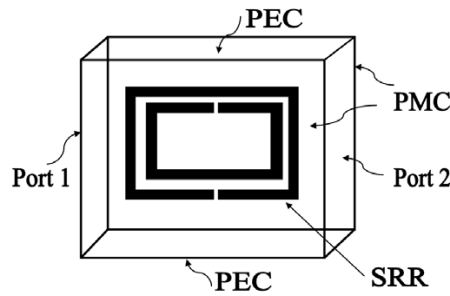


**Figure 12.** Waveguide setup to extract  $S$ -parameter of the split ring resonator.

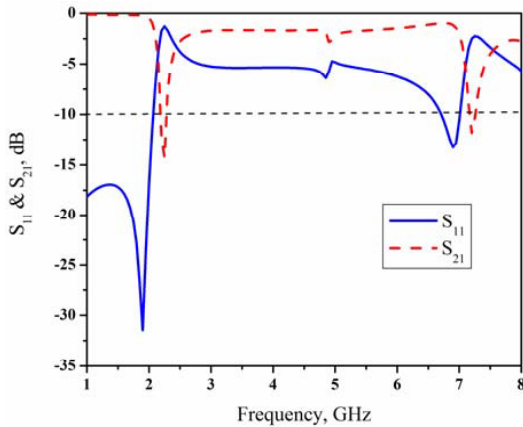


**Figure 13.** Extracted  $S$ -parameter of the split ring resonator.

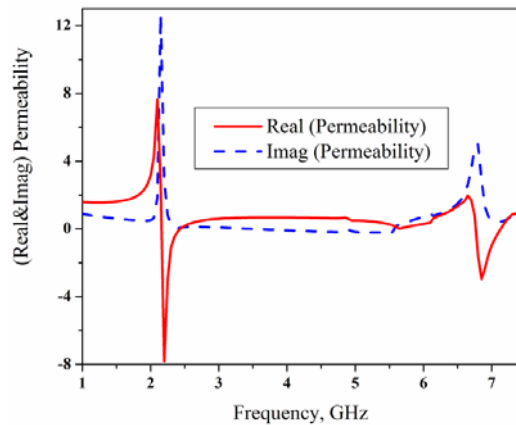


**Figure 14.** Extracted negative permeability of the proposed SRR resonator.

perfect magnetic field (PMC) is assigned at the top and bottom of the waveguide, and perfect electric field (PEC) is assigned in ( $X$ -axis) and the incident plane wave (Port 1, 2) assigned remaining side of wave guide ( $Z$ -axis). The retrieved  $S_{11}$  and  $S_{21}$  parameters are plotted as shown in Figure 13.

It shows the presence of two negative bands at 2.4 and 7.4 GHz, where the  $S_{21}$  value is  $< -10$  dB, and  $S_{11}$  value is  $< -3$  dB. To confirm the presence of negative permeability and permittivity, the extracted  $S$ -parameter ( $S_{21}$  and  $S_{11}$ ) values are used based on smith et al. [24] method. The obtained real and imaginary permeability values are depicted in Figure 14, which represents the two negative permeability characteristics at 2.4 and 7.4 GHz, and these properties are the reason for performance enhancement of the proposed antenna.

The proposed antenna radiation characteristics for various frequencies at 2.4, 5.2 and 8.2 GHz are shown in Figures 15(a) and 15(b) for  $H$ -plane and  $E$ -plane. Almost omnidirectional and eight-shaped radiation patterns are exhibited by the antenna for  $H$ -plane and  $E$ -plane, respectively.

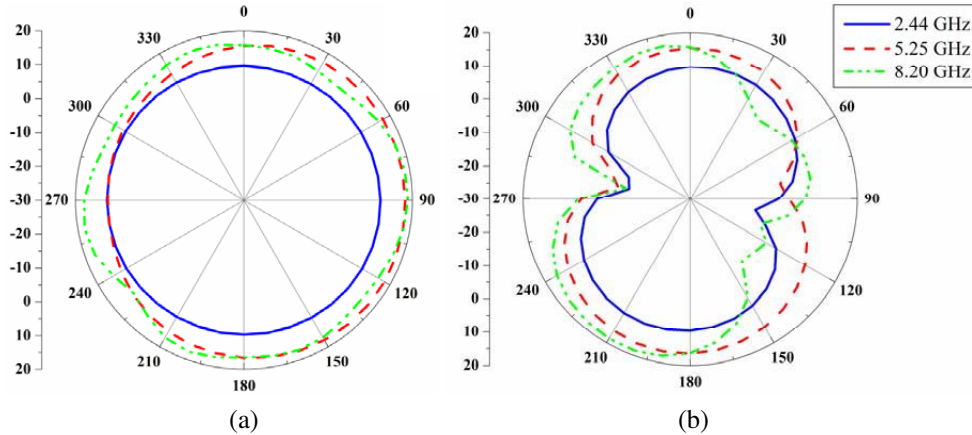


**Figure 15.** The radiation characteristics of the proposed antenna at 2.44, 5.2 and 8.2 GHz. (a)  $H$ -plane and (b)  $E$ -plane.

In  $E$ -plane ( $X$ - $Y$ ), radiation patterns are tilted. In 8.2 GHz, radiation pattern shape worsens due to asymmetric coplanar ground structure which has impact on higher frequencies. The proposed antenna has a gain of 0.567 dBi at 2.4 GHz lower band, whereas at higher frequencies 1.40 dBi for 5.25 GHz and 1.90 dBi for 8.2 GHz. The gain of the proposed antenna is low due to the small size of the antenna which is achieved through this design.

## 6. CONCLUSION

In this paper, a compact ACS-fed monopole antenna is presented for a multiband operation. The three branches help to obtain multiband characteristics, and loaded SRR structure aids in improving the antenna performances such as impedance matching and size reduction. The proposed antenna has achieved the fractional bandwidth of 8.26, 12.12 and 8.41% for the three desired frequency bands and covers WLAN, WiMAX and ITU band applications. The combination of ACS-fed and SRR-based technique could be used to achieve more size reduction and impedance matching. This makes the proposed antenna suitable for future wireless communications.

## REFERENCES

1. Liu, W., C. Wu, and N. Chu, "A compact CPW-fed slotted patch antenna for dual-band operation," *IEEE Antennas and Wireless Letters*, Vol. 9, 110–113, 2010.
2. Liu, W. C. and W. R. Chen, "CPW-fed compact meandered patch antenna for dual-band operation," *Electronics Letters*, Vol. 40, 1–2, 2004.
3. Xu, P., Z. Yan, and C. Wang, "Multi-band modified fork-shaped monopole antenna with dual L-shaped parasitic plane," *Electronics Letters*, Vol. 47, 47–48, 2011.
4. Sujith, R., V. Deepu, D. Laila, C. K. Aanandan, and K. Vasudevan, "A compact dual-band modified T-shaped CPW-fed monopole antenna," *Microw. Opt. Technol. Lett.*, Vol. 51, 937–939, 2009.

5. Tsai, L., "A dual-band bow-tie-shaped CPW-fed slot antenna for WLAN applications," *Progress In Electromagnetics Research C*, Vol. 47, 167–171, 2014.
6. Sayidmarie K. H. and T. A. Nagem, "Compact dual-band dual-ring printed mono-pole antennas for WLAN applications," *Progress In Electromagnetics Research B*, Vol. 43, 313–331, 2012.
7. Deepu, V., R. K. Raj, M. Joseph, M. N. Suma, and P. Mohanan, "Compact asymmetric coplanar strip fed monopole antenna for multiband applications," *IEEE Transactions on Antennas Propag.*, Vol. 55, 2351–2357, 2007.
8. Li, X., X. W. Shi, W. Hu, P. Fei, and J. F. Yu, "Compact triband ACS-fed monopole antenna employing open-ended slots for wireless communication," *IEEE Antennas Wirel. Propag. Lett.*, Vol. 12, 388–391, 2013.
9. Song, Y., Y. C. Jiao, X. M. Wang, Z. B. Weng, and F. S. Zhang, "Compact coplanar slot antenna fed by asymmetric coplanar strip for 2.4/5 GHz WLAN operations," *Microw. Opt. Technol. Lett.*, Vol. 50, 3080–3083, 2008.
10. Li, B., Z. Yan, and T. Zhang, "Triple-band slot antenna with U-shaped open stub fed by asymmetric coplanar strip," *Progress In Electromagnetics Research Letters*, Vol. 37, 123–131, 2013.
11. Chen, L., Y. Luo, and Y. Zhang, "Compact tri-band planar monopole antenna with ACS-fed structure," *Progress In Electromagnetics Research Letters*, Vol. 49, 45–51, 2014.
12. Deepu, V., R. Sujith, S. Mridula, C. K. Aanandan, K. Vasudevan, and P. Mohanan, "ACS fed printed F-shaped uniplanar antenna for dual band WLAN applications," *Microw. Opt. Technol. Lett.*, Vol. 51, 1852–1856, 2009.
13. Liu, Y., P. Wang, and H. Qin, "A compact triband ACS-fed monopole antenna employing inverted-L branches for WLAN /WiMAX applications," *Progress In Electromagnetics Research C*, Vol. 47, 131–138, 2014.
14. Naidu, P., V. A. Malhotra, and R. Kumar, "A compact ACS-fed dual-band monopole antenna for LTE, WLAN/WiMAX and public safety applications," *Microsyst. Technol.*, 1–8, 2015.
15. Naidu P. V. and A. Malhotra, "A small ACS-fed tri-band antenna employing C and L shaped radiating branches for LTE/WLAN/WiMAX/ITU wireless communication applications," *Analog Integr. Circuits Signal Process.*, Vol. 85, 489–496, 2015.
16. Li, Y., W. Li, and Q. Ye, "A compact asymmetric coplanar strip-fed dual-band antenna for 2.4/5.8 GHz WLAN applications," *Microw. Opt. Technol. Lett.*, Vol. 55, 2066–2070, 2013.
17. Smith, D. R., W. J. Padilla, D. C. Vier, S. C. Nemat-Nasser, and S. Schultz, "Composite medium with simultaneously negative permeability and permittivity," *Phys. Rev. Lett.*, Vol. 84, 4184–4187, 2000.
18. Baena, J. D., J. Bonache, F. Martín, R. M. Sillero, F. Falcone, T. Lopetegi, M., A. G. Laso, J. G. García, I. Gil, M. F. Portillo, M. Sorolla, and S. Member, "Equivalent-circuit models for split-ring resonators and complementary split-ring resonators coupled to planar transmission lines," *IEEE Trans. Microw. Theory Tech.*, Vol. 53, 1451–1461, 2005.
19. Ntaikos, D. K., N. K. Bourgis, and T. V. Yioultis, "Metamaterial-based electrically small multiband planar monopole antennas," *IEEE Antennas Wirel. Propag. Lett.*, Vol. 10, 963–966, 2011.
20. Kang, L., H. Wang, X. H. Wang, and X. Shi, "Compact ACS-fed monopole antenna with rectangular SRRs for tri-band operation," *Electron. Lett.*, Vol. 50, 1112–1114, 2014.
21. Ansal, K. A. and T. Shanmuganantham, "A novel CB ACS-fed dual band antenna with truncated ground plane for 2.4/5 GHz WLAN application," *AEU — Int. J. Electron. Commun.*, Vol. 69, 1506–1513, 2015.
22. Simons, R. N., *Coplanar Waveguide Circuits, Components and Systems*, John Wiley & Sons, 2004.
23. Chen, H., J. Zhang, Y. Bai, Y. Luo, L. Ran, Q. Jiang, et al., "Experimental retrieval of the effective parameters of metamaterials based on a waveguide method," *Opt. Express*, Vol. 14, 12944–9, 2006.
24. Smith, D. R., S. Schultz, P. Markos, and C. M. Soukoulis, "Determination of negative permittivity and permeability of metamaterials from reflection and transmission coefficients," *Phys. Rev. B*, Vol. 65, 195104–9, 2002.